

Discontinuous bifurcation and coexistence of attractors in a piecewise linear map with a gap*

Qu Shi-Xian(屈世显)^{a)†}, Lu Yong-Zhi(卢永智)^{a)},
Zhang Lin(张林)^{a)}, and He Da-Ren(何大韧)^{b)}

^{a)}*Institute of Theoretical & Computational Physics, School of Physics and Information Technology,
Shaanxi Normal University, Xi'an 710062, China*

^{b)}*College of Physics Science and Technology, Yangzhou University, Yangzhou 225002, China*

(Received 18 March 2008; revised manuscript received 26 March 2008)

Coexistence of attractors with striking characteristics is observed in this work, where a stable period-5 attractor coexists successively with chaotic band-11, period-6, chaotic band-12 and band-6 attractors. They are induced by different mechanisms due to the interaction between the discontinuity and the non-invertibility. A characteristic boundary collision bifurcation, is observed. The critical conditions are obtained both analytically and numerically.

Keywords: coexistence of attractors, piecewise linear map, mapping hole, discontinuous bifurcation

PACC: 0545

1. Introduction

Recently, there has been a considerable interest in the dynamics of piecewise continuous maps with gaps.^[1–5] The reason lies in the fact that they can describe many practical systems that often display certain kinds of catastrophes, crises, or extreme events. These systems may include models of nerve cells or cardiopathy,^[6–8] relaxation and impact oscillators,^[4,5,9–13] relay control systems,^[14] DC-DC converters,^[14–18] and many others. The discontinuities in a map divide the phase space into individual zones of different dynamical features. The interactions among them may trigger dynamical phenomena with new characteristics. The bifurcations induced by the discontinuity which show new characteristics are generally addressed as border-collision bifurcations.^[19,20] The situation becomes more complicated when the discontinuity and the non-invertibility emerge simultaneously in a system. The interplay between these two properties can produce very different behaviours compared with those observed in systems that are smooth everywhere. Two of us (He and Qu) and co-workers have studied some relaxation oscillators^[11–13,21–27] and presented a detailed description of an electronic relaxation oscillator in Ref.[11]. The interesting phenomena observed in these systems include type V intermittencies,^[11,21] crises in-

duced by collision of attractors with discontinuities or mapping holes,^[23–25] multiple Devil's staircases,^[26,27] coexistence of attractors,^[12,22] and many others.^[28,29]

In this paper, we report our observation on a series of characteristic coexistence of a period-5 orbit with different types of attractors (periodic or chaotic attractors). Section 2 shows the model and system employed in the work. The results and discussion are presented in Section 3, and the conclusions drawn from this work are given in Section 4.

2. Model and system

The model employed in this work is a both discontinuous and non-invertible piecewise linear map. It is a simplified model for a relaxation oscillator, in which a hole-induced crisis^[11,23–25] was observed. The mapping function reads

$$x_{n+1} = f_i(x_n) = k_i \cdot x_n + b_i \pmod{1} \quad (1)$$

where $i=1,2,3,4$, and

$$\begin{aligned} k_1 &= \frac{y_b - y_A}{x_b - x_A}, \quad b_1 = y_A, \quad x \in [x_A, x_b]; \\ k_2 &= \frac{y_C - y_b}{x_g - x_b}, \quad b_2 = y_b - k_2 x_b, \quad x \in [x_b, x_g]; \\ k_3 &= \text{constant}, \quad b_3 = \text{constant}, \quad x \in [x_g, x_F]; \\ k_4 &= \text{constant}, \quad b_4 = \text{constant}, \quad x \in [x_F, x_G] \end{aligned}$$

*Project supported by the National Natural Science Foundation of China (Grant No 10275053).

†Corresponding author. E-mail: sxqu@snnu.edu.cn

<http://www.iop.org/journals/cpb> <http://cpb.iphy.ac.cn>

with $y_b = b_1 - \mu$, where μ is selected as the control parameter. The values of the other parameters are selected as $y_A = 0.0203921$, $y_C = 0.460000$, $y_G = y_A$, $x_A = 0$, $x_b = 0.107663$, $x_g = 0.350000$, $x_F = 0.497121$, $x_G = 1$, $k_3 = 3.07055$, $b_3 = -0.530165$, $k_4 = 0.405507$, and $b_4 = -0.201586$.

3. Results and Discussion

First of all, the bifurcation diagram for parameter $\mu \in [0.025, 0.065]$ is investigated and plotted in Fig.1. It demonstrates that a stable period-5 (P-5) attractor coexists, in turn, with other types of attractors, i.e.

- $\mu_{c_1} \leq \mu < \mu_{c_2}$: coexisting with band-11 chaos;
- $\mu_{c_3} \leq \mu < \mu_{c_4}$: coexisting with P-6;
- $\mu_{c_4} \leq \mu < \mu_{c_5}$: coexisting with band-12 chaos;
- $\mu_{c_5} \leq \mu < \mu_{c_6}$: coexisting with band-6 chaos;
- $\mu_{c_6} \leq \mu$: no coexistence

with $\mu_{c_1} = 0.02879$, $\mu_{c_2} = 0.03040$, $\mu_{c_3} = 0.03952$, $\mu_{c_4} = 0.04506$, $\mu_{c_5} = 0.05011$, $\mu_{c_6} = 0.05114$.

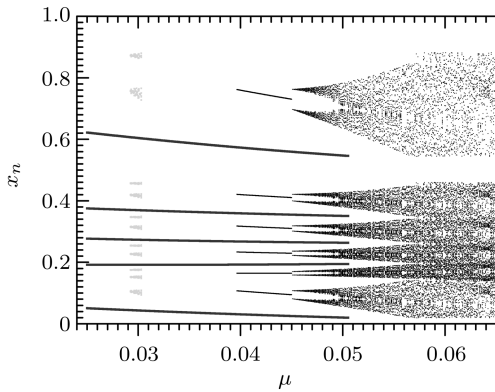


Fig.1. Bifurcation diagram.

In order to describe the occupation status of the basin of the P-5 attractor, we define the phase space volume fraction

$$v_{P5} = \frac{N_{P5}}{N_0} \quad (2)$$

by tracking N_0 independent iteration sequences with their initial trajectories randomly selected in the phase space. Here, N_{P5} is the number of sequences in which the trajectories are attracted to the P-5 orbit. The dependences of the volume fraction of the P-5 attractor and the Lyapunov exponent on the control parameter

μ are plotted in Fig.2. They exhibit very good correspondence with the bifurcation diagram. The mechanisms that induce and destroy these coexistences are explained in the following subsections.

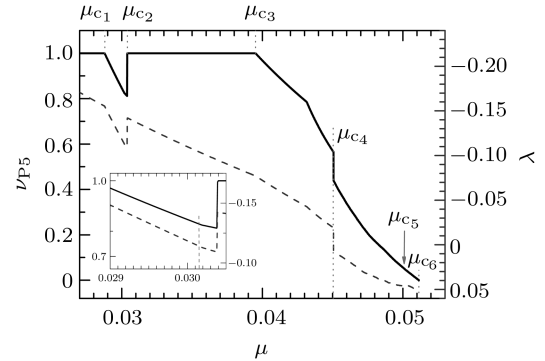


Fig.2. Volume fraction and Lyapunov exponent, where the solid line denotes the volume fraction of the basin of the P-5 attractor, and the dashed line represents the Lyapunov exponent.

3.1. Mapping hole due to discontinuity

As one can see in Fig.3, there is a gap at x_g which defines a forbidden zone,^[12] and an overlap range between y_A and y_b . The former defines the discontinuity, and the latter the non-invertibility. The minimum (x_b, y_b) of the mapping function and its first to fourth-fold backward images at images at $f^{-1}(x_b)$, $f^{-2}(x_b)$, $f^{-3}(x_b)$ and $f^{-4}(x_b)$, respectively, determine the five minima in the corresponding 5-fold mapping $f^5(x)$ (we only marked two of these positions, i.e., x_b and $f^{-1}(x_b)$, by the dashed lines in the figure). The minima are important for analysing the appearance and the disappearance of the attractors coexisting with the P-5.

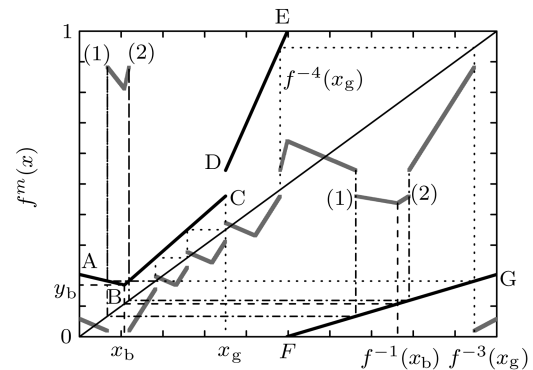


Fig.3. Schematic plot of the mapping hole, where the thick lines represent the mapping function, the thick grey lines show the 5-fold map, the dashed lines connect x_b and its first-fold backward images, the dotted lines connect the trival backward-images of x_g , and the dash-dotted lines confine the two holes.

x_g and its backward images via branches BC, FG and DE, i.e. $f^{-1}(x_g)$, $f^{-2}(x_g)$, $f^{-3}(x_g)$ and $f^{-4}(x_g)$, are connected via the dotted lines. They divide the phase space into five zones, and in each of them, one piece of the 5-fold map is defined. We call the discontinuities (gaps) appearing at these points the trivial ones. There are still two other 3-fold backward images of x_g since $f^{-2}(x_g)$ falls in the overlap range. They are $f^{-3}(x_g)_1 \equiv f_1^{-1}f_2^{-2}(x_g)$ and $f^{-3}(x_g)_2 \equiv f_2^{-3}(x_g)$, marked respectively by '(1)' and '(2)' around x_b in the figure. Their 4-fold counterparts are $f^{-4}(x_g)_1$ and $f^{-4}(x_g)_2$, positioned around $f^{-1}(x_b)$ and also marked by '(1)' and '(2)', respectively. The 5-fold mapping at positions $f^{-3}(x_g)_1$ and $f^{-3}(x_g)_2$ produces a pair of gaps of the same size. The small piece of the map between them is then cut off by them and falls downward to form the first hole around x_b . Similarly, the pair of gaps positioned at $f^{-4}(x_g)_1$ and $f^{-4}(x_g)_2$ gives rise to the second hole at the bottom of the 5-fold map around the minimum at $f^{-1}(x_b)$. Thus, we have altogether two holes due to the interaction between the discontinuity and the non-invertibility, which often induces new phenomena in the mapping systems of this kind.^[21–29] The crisis reported in Ref.[23] appears at $\mu = 0.0565359$ (see the bifurcation diagram), which is the result of the collision between a band-6 chaotic attractor and a hole in the 6-fold map. In the current work, however, the mapping holes serve as the mechanism for the coexistence of attractors.

Before going further, we need to analyse the stability condition for the P-5 orbit (the intersections between the 5-fold map and the diagonal in Fig.3), which is defined by the fixed-points equation

$$f_2^2 f_1 f_3 f_4(x^*) = x^*. \quad (3)$$

The stability condition reads

$$|k_1 k_2^2 k_3 k_4| < 1, \quad (4)$$

which holds in the entire parameter range of Fig.1. Unfortunately, the P-5 orbit is no longer allowed when it collides with the boundary of the forbidden zone. The critical parameter μ_{c_6} is calculated from the criterion

$$x^* = x_g^+, \quad (5)$$

where the superscript '+' implies that the P-5 trajectory x^* collides with x_g from the right side.

3.2. Coexistence of P-5 and chaotic band-11 attractors

The appearance or the disappearance of the holes depends on μ . The backward images of x_g in Fig.3 is single valued as $\mu < \mu_{c_1}$, where $y_b > f^{-2}(x_g)$; thus, the holes disappear. We have only the trivial discontinuities intersecting the diagonal at $f^{-3}(x_g)$, $f^{-2}(x_g)$, $f^{-1}(x_g)$, x_g and $f^{-4}(x_g)$, respectively. They serve as repellers of iterates, just like unstable fixed points, and may be viewed as the boundary of the basin of the P-5 attractor. We can analytically prove that the corresponding minima at x_b , $f^{-4}(x_b)$, $f^{-3}(x_b)$, $f^{-2}(x_b)$ and $f^{-1}(x_b)$ are higher than the intersections between the diagonal and these trivial discontinuities. Therefore, the trajectories passing through the small pieces of the phase space near these minima will be definitely attracted to a neighbouring stable fixed point, i.e. the P-5 orbit. Consequentially, the basin of the P-5 attractor occupies the entire phase space. The opposite tendency appears when $\mu > \mu_{c_1}$, where $y_b \leq f^{-2}(x_g)$ in Fig.4. Two holes then appear

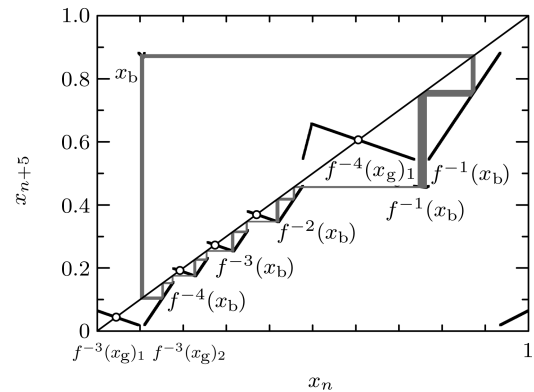


Fig.4. The 5-fold map for $\mu = 0.02950$, where the P-5 attractor is marked by the circles, and the coexisting chaotic band-11 attractor is shown by the grey line. The former is obtained by the iteration with initial trajectory $x_0 = 0.04$, but the latter with $x_0 = 0.76$. The first 106 iterations are dropped to avoid transients in each case.

in the 5-fold map; however, the P-5 orbit remains stable. The nontrivial discontinuities corresponding to the two holes intersect the diagonal at $f^{-3}(x_g)_1$, $f^{-3}(x_g)_2$, $f^{-4}(x_g)_1$ and $f^{-4}(x_g)_2$, and behave like unstable fixed points. The trajectories passing through the small pieces of phase space near the minima will no longer be attracted to the original P-5 attractor, but escape through the holes. Therefore, part of phase space is cut out of the original basin of the P-5 attractor and left for another attractor. In this case, a band-

11 chaotic attractor appears in the cut off portion, as shown by the grey lines in Fig.4. The coexistence of the P-5 and the band-11 attractors is then observed. The basin of this new attractor is expressed analytically as

$$B \equiv \lim_{n \rightarrow \infty} \sum_{i=1}^n f^{-i} [f^{-3}(x_g)_2 - f^{-3}(x_g)_1]. \quad (6)$$

Obviously, the boundary between the basins of the two attractors is intertwined. The basin of this chaotic attractor expands when μ increases, and so does the attractor itself. The volume fraction of the basin of the P-5 orbit thus decreases, and this is shown in Fig.2 by v_{P5} . When μ is close to the second critical point μ_{c_2} , the decrease of the volume fraction of the basin of the P-5 orbit and the increase of the Lyapunov exponent of the system slow down as shown by the inset in Fig.2. The magnitude of the slope of the former decreases by about 50%, but that of the latter is only about 32%, if we can approximate their variations by linear relations. This means that the expanding of the basin of the chaotic attractor is slower than that of the attractor itself. Therefore, at the critical point μ_{c_2} , the trajectories from the chaotic attractor run into the basin of the P-5 attractor and are thus attracted by the latter. The volume of the basin of the chaotic attractor shrinks to zero. The coexistence dies out, and thus the basin of the P-5 attractor exclusively occupies the entire phase space again. The criteria for this collision can be easily found in Fig.4, i.e. the 10-fold image of the minimum positioned at x_b is lower than the intersection between the diagonal and the left boundary of the second hole. Therefore, the critical parameter μ_{c_2} is determined by solving the following equation:

$$f_3 f_2^3 f_4 f_3 f_2^4(x_b) \leq f^{-4}(x_g)_1. \quad (7)$$

3.3. Coexistence of P-5 and P-6

The coexisting of the P-5 and the P-6 attractors occurs when μ tends to the third critical point μ_{c_3} . To clearly show the mechanism, we plot the 6-fold map for $\mu = \mu_{c_3}$ in Fig.5, where the bottom tips, i.e. the six minima of the 6-fold mapping function collide with the diagonal. The critical condition can be simply cal-

culated from

$$f_4 f_3 f_2^4(x_b) = x_b. \quad (8)$$

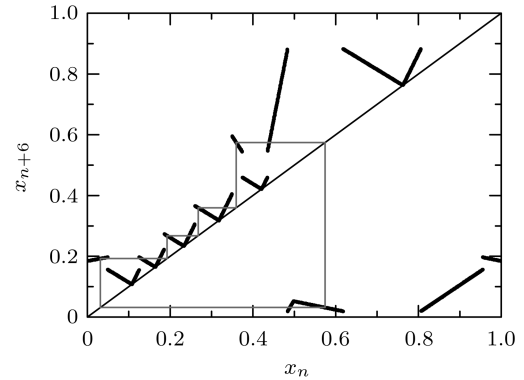


Fig.5. The 6-fold map for $\mu = \mu_{c_3}$, where the P-5 trajectories are marked by the grey line, the initial trajectory is $x_0 = x_g$, and the first 10^6 are dropped to avoid transients. The coexisting P-6 attractor is shown by the contact points between the six minima and the mapping.

As one can see, there are six V-type valleys in the figure. When $\mu > \mu_{c_3}$, each of the six valleys intersects the diagonal at a stable fixed point, x_M^* , on the left side of the minimum and an unstable one, x_u^* , on the right side. This bifurcation is similar to a tangent bifurcation but cannot be classified into it because the mapping function is not smooth at these minima, and their tangents are not defined. The equations of the fixed points and the derivatives of the local mapping at these points can be easily derived due to the piecewise linear property of the map. We only list the ones for the right most valley, i.e.

$$\begin{aligned} x_M^* &= \frac{\sum_{n=0}^7 p_n^M \mu^n}{\sum_{n=0}^7 q_n^M \mu^n}, & f'[x_M^*] &= k_1 k_2^3 k_3 k_4 < 0; \\ x_u^* &= \frac{\sum_{n=0}^7 p_n^u \mu^n}{\sum_{n=0}^7 q_n^u \mu^n}, & f'[x_u^*] &= k_2^4 k_3 k_4 > 0. \end{aligned} \quad (9)$$

The coefficients in these equations are listed in Table.1. Clearly, the left fixed point is stable but the right one is unstable. The variations of these fixed points versus the control parameter are shown in Fig.6. One finds that the two fixed points approach each other as μ decreases from μ_{c_4} . They collide with each other to form a tip when μ reaches μ_{c_3} , and then the stable one loses stability simultaneously. The two fixed points have different derivatives at $\mu = \mu_{c_3}$. This bifurcation is a kind of border-collision bifurcation,^[19,20] and can also be catalogued as discontinuous fold bifurcation.^[30,31]

Table 1. The coefficients for Eq.(9).

n	p^M	q^M	p^u	q^u
0	7.38778×10^{-3}	6.79588×10^{-3}	6.11490×10^{-3}	3.48748×10^{-2}
1	-1.93212×10^{-1}	-1.15769×10^{-1}	1.32591	4.60718×10^{-1}
2	-1.92365	-2.96562	-36.8405	-44.1910
3	-18.7600	-47.3912	-567.901	-532.971
4	-138.042	-342.578	-3202.36	-2698.45
5	-532.553	-1215.86	-9204.79	-7262.84
6	-998.653	-2125.10	-13665.4	-10343.4
7	-740.590	-1489.76	-8362.02	-6147.47

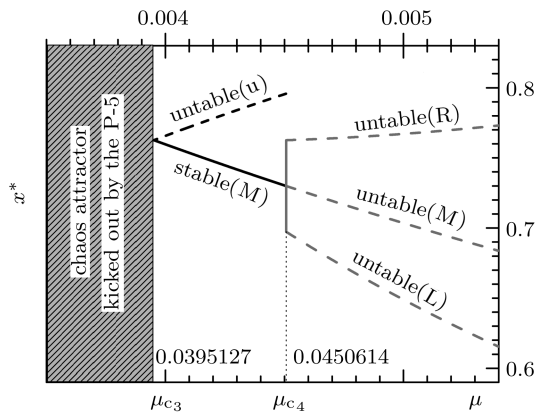


Fig.6. Discontinuous bifurcations for the local map, where parameters ‘u’ and ‘M’ denote the fixed points x_u and x_M , and ‘L’ and ‘R’ represent the fixed points x_L and x_R , respectively.

3.4. Coexistence of P-5 and chaotic band-12 attractors

The last nontrivial coexistence appears at μ_{c_4} where the P-6 attractor previously coexisting with the P-5 abruptly transits into a band-12 chaos, but the P-5 attractor remains stable (see Fig.1). The mechanism can be easily understood by a 12-fold mapping in which there are twelve equivalent valleys intersecting the diagonal. We can analytically obtain this map. Only the key portion of the right most valley is drawn in Fig.7 for three different control parameters near the critical value. When $\mu < \mu_{c_4}$, the straight line connecting points A and B in Fig.7(a) intersects the diagonal at x_M^* , a stable fixed point. The line coincides with the diagonal when $\mu = \mu_{c_4}$, and thus we have an infinite number of fixed points bounded by end points A and B in Fig.7(b). Those two ends are also the intersections between the diagonal and lines DA and BC. They are two fixed points, denoted by x_L^* and x_R^* , respectively. The periodic doubling bifurcation here produces two fixed points separated by a

non-zero distance. We emphasize that these two fixed points are intrinsically unstable. They lose stability immediately after an infinitesimal increase of μ from the critical value μ_{c_4} . Figure 7(c) displays that the fixed points are unstable when $\mu \geq \mu_{c_4}$. Hence, one cannot observe any period-12 orbit but for a band-12 chaos. This coexistence ends up with the coexistence of the P-5 and the chaotic band-6 attractors when $\mu \geq \mu_{c_5}$.

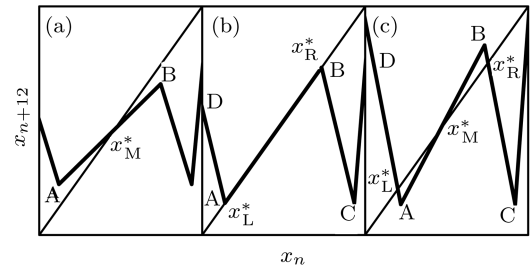


Fig.7. 12-fold map to display the rectangular-fork bifurcation, where (a) $\mu = 0.0398 < \mu_{c_4}$, x_n -axis : [0.7580, 0.7642], x_{n+12} -axis : [0.7580, 0.7642]; (b) $\mu = \mu_{c_4}$ x_n -axis : [0.6820, 0.7920], x_{n+12} -axis : [0.6820, 0.7920]; (c) $\mu = 0.0500 > \mu_{c_4}$, x_n -axis : [0.6060, 0.8200], x_{n+12} -axis : [0.6060, 0.8200].

The control parameter dependence of the three fixed points, x_M^* , x_L^* and x_R^* , corresponding to the above mentioned bifurcation that induces the direct transition from a P-6 to a chaotic band-12 attractor is plotted in Fig.6. It shows a very different kind of periodic doubling bifurcation from the conventional ones,^[32] in which the ‘newly born’ fixed points are separated from each other by a non-zero distance as the control parameter goes beyond its critical value. Nevertheless, the Lyapunov exponent of the system changes discontinuously at this critical point (see Fig.2). The new fixed points emerging after this bifurcation could, in general, be either stable or unstable. However, both of them are unstable in the current work. This bifurcation can, of course, be classified as a discontinuous bifurcation^[30] in the sense

that the number of the fixed points or the Jacobian of the map undergoes a discontinuous change when the control parameter passes through the critical value. Yet we employ ‘discontinuous’ here to emphasize the non-zero-distance separation of the newly born fixed-points pair in the phase space.

Considering the fact that A and B are the boundaries of the local map, this bifurcation scenario can also be viewed as a periodic doubling bifurcation immediately followed by a boundary-collision bifurcation. It is a particular subclass of the boundary-collision bifurcation. This behaviour is very similar to the bifurcations observed in DC-DC converters^[2,3] and two-block stick-slip systems,^[32] where a conventional periodic doubling occurs when a stable fixed point loses stability, producing a period-2 orbit; the

system bursts into chaos when this periodic orbit collides with the non-smooth boundary.

4. Conclusions

We have found that a stable period-5 attractor coexists with a sequence of chaotic and periodic attractors. The interplay between the discontinuity and the non-invertibility is responsible for these characteristic coexistence phenomena. The mechanisms for their emerging and vanishing are discussed and analysed in detail. The critical parameters are calculated both analytically and numerically, and the agreement is excellent. A characteristic bifurcation, is observed. It provides a particular case for the boundary collision bifurcations.

References

- [1] Hogan S J, Higham L and Griffin T C L 2007 *Proc. R. Soc. A* **463** 49
- [2] Jain P and Banerjee S 2003 *Int. J. Bifurcat. Chaos* **13** 3341
- [3] Banerjee S, Parui S and Gupta A 2004 *IEEE Trans. Circ. Systems II* **51** 649
- [4] Jin L, Lu Q S and Twizell E H 2006 *J. Sound and Vibration* **298** 1019
- [5] Budd C J and Piiroinenb P T 2006 *Physica D* **220** 127
- [6] Glass L 1991 *Chaos* **1** 13
- [7] Glass L and Belair J 1986 *Lect. Notes Biomath.* **66** 232
- [7] Holden A V and Fan Y 1992 *Chaos, Solitons Fractals* **2** 349
- [8] Grudzinski K and Zebrowski Jain J 2004 *Physica A* **336** 153
- [9] Alström P and Levinson M T 1988 *Phys. Lett. A* **128** 187
- [10] Lamba H and Budd C J 1994 *Phys. Rev. E* **50** 84
- [11] He D R, Wang B H, Bauer M, Habip S, Krueger U, Martienssen W and Christiansen B 1994 *Physica D* **79** 335
- [12] Guan S, Wang B H, Wang D K and He D R 1995 *Phys. Rev. E* **52** 453
- [13] Wang J, Ding X L, Hu Bambi Hu, Wang B H, Mao J S and He D R 2001 *Phys. Rev. E* **64** 026202
- [14] Zhusubaliyev Z T and Mosekilde E 2003 *Bifurcation and Chaos in Piecewise-Smooth Dynamical Systems* (Singapore: World Scientific)
- [15] Fang J Q, Luo X S, Wang B H and Zhao Y B 2005 *Acta Phys. Sin.* **54** 5022 (in Chinese)
- [16] Chen G R, Fang J Q, Jiang P Q, Luo X S, Quan H J, Wang B H and Zou Y L 2003 *Acta Phys. Sin.* **52** 12 (in Chinese)
- [17] Dai D, Ma X K and Li X F 2003 *Acta Phys. Sin.* **52** 2729 (in Chinese)
- [18] Ren H P and Liu D 2005 *Chin. Phys.* **14** 1352
- [19] Nusse H E and Yorke J A 1992 *Physica D* **57** 39
- [19] Nusse H E and Yorke J A 1995 *Int. J. Bifurc. Chaos* **5** 189
- [20] Nusse H E, Ott E and Yorke J A 1994 *Phys. Rev. E* **49** 1073
- [21] He D R, Bauer M, Habip S, Krueger U, Martienssen W, Christiansen B and Wang B H 1992 *Phys. Lett. A* **171** 61
- [22] He D R, Ding E J, Bauer M, Habip S, Krueger U, Martienssen W and Christiansen B 1994 *Europhys. Lett.* **26** 165
- [23] Qu S X, Christiansen B and He D R 1995 *Phys. Lett. A* **201** 413
- [24] Qu S X, Christiansen B and He D R 1995 *Acta Phys. Sin.* **44** 841 (in Chinese)
- [25] He Y, Jiang Y M, Shen Y and He D R 2004 *Phys. Rev. E* **70** 056213
- [26] Qu S X, Wu S G and He D R 1998 *Phys. Rev. E* **57** 402
- [27] Qu S X, Wu S G and He D R 1997 *Phys. Lett. A* **231** 152
- [28] Dai J, Ding X L and He D R 2006 *Acta Phys. Sin.* **55** 3979 (in Chinese)
- [29] He D R, Mao X Y, Qu S X and Wu S G 1997 *Acta Phys. Sin.* **46** 1464 (in Chinese)
- [30] Leine R I, Van Campen D H and Van De Vrande B L 2000 *Int. J. Nonlinear Dyn. Chaos Eng. Syst.* **23** 105
- [31] Galvanetto U 2004 *J. Sound and Vib.* **276** 121
- [32] Schuster H G and Just W 2005 *Deterministic Chaos* (Weinheim: Wiley-VCH)